

**Synthesis and stability of hydrogen iodide at high pressures**

HPSTAR  
453-2017

 Jack Binns,<sup>1</sup> Xiao-Di Liu,<sup>2</sup> Philip Dalladay-Simpson,<sup>1</sup> Veronika Afonina,<sup>3</sup> Eugene Gregoryanz,<sup>1,2,3</sup> and Ross T. Howie<sup>1,\*</sup>
<sup>1</sup>*Center for High Pressure Science Technology Advanced Research, Shanghai, People's Republic of China*
<sup>2</sup>*Key Laboratory of Materials Physics, Institute of Solid State Physics, Chinese Academy of Sciences, Hefei, People's Republic of China*
<sup>3</sup>*Centre for Science at Extreme Conditions and School of Physics and Astronomy, University of Edinburgh, Edinburgh EH9 3JZ, United Kingdom*

(Received 7 August 2017; published 11 October 2017)

Through high-pressure Raman spectroscopy and x-ray diffraction experiments, we have investigated the formation, stability field, and structure of hydrogen iodide (HI). Hydrogen iodide is synthesized by the reaction of molecular hydrogen and iodine at room temperature and at a pressure of 0.2 GPa. Upon compression, HI solidifies into cubic phase I, and we present evidence for the emergence of a phase I' above 3.8 GPa. Across the wide temperature regime presented here, HI is unstable under compression (11 GPa at 300 K, 18 GPa at 77 K), decomposing into its constituent elements, after which no further reaction between hydrogen and iodine was observed up to pressures of 60 GPa. This study provides both the constraints on the phase diagram of HI and its kinetic stability.

DOI: [10.1103/PhysRevB.96.144105](https://doi.org/10.1103/PhysRevB.96.144105)**I. INTRODUCTION**

The high-pressure behavior of molecular systems containing the simplest and most abundant element, hydrogen, have been the subject of an intense experimental and theoretical effort, perhaps best exemplified by the presumed insulator-to-metallic transition expected in elemental H<sub>2</sub> [1–4]. On the other hand, investigations into the pressurization of hydrogen-bearing species have received a significant impetus by the recent claim of high-temperature superconductivity in hydrogen sulfide (H<sub>2</sub>S) at unprecedented high temperatures [5]. Hydrogen iodide (HI) has been proposed to exhibit both these phenomena at high pressures and low temperatures, with a claimed insulator-to-metallic transition at 50 GPa [6,7]. Additionally, compounds of HI-H<sub>2</sub> have been recently predicted to be stable above 50 GPa, with superconducting phases emerging above 100 GPa with a  $T_c \leq 17.5$  K [8,9].

The hydrogen halides HCl, HBr, and HI follow a law of corresponding states and exhibit a similar solid phase sequence at ambient pressure and low temperature. Phase I at high temperatures adopts a cubic structure ( $Fm\bar{3}m$ ) with halogen atoms forming a fcc lattice with hydrogens either in twelvefold disordered positions or rotating unhindered about these sites [10–12]. The structure of phase II, existing at intermediate temperatures, remained unresolved until neutron diffraction revealed a structure containing linear chains of twofold disordered H-X...H hydrogen bonds [11,13]. The low-temperature/high-pressure phase III in HCl and HBr adopts a proton-ordered orthorhombic structure ( $Cmc2_1$ ) containing zigzag chains of H-X...H hydrogen bonds [11,14]. Phase III in HI adopts a triclinic structure ( $P\bar{1}$ ) with stacked layers of hydrogen-bonded squares [11]. This difference is due to changes in the relative strengths of the two competing intermolecular interactions: the halogen-halogen bonding, which increases in strength from Cl to I, and the reciprocal decrease in hydrogen bonding strength [15].

An additional phase I' exists for HBr but not for HCl, HI, or DBr. This phase is characterized by slight changes in the Raman spectra with neutron diffraction showing a transition from a spherical hydrogen scattering density in phase I to a toroidal distribution oriented about the  $\langle 111 \rangle$  cubic axes [12,16].

The instability of HI, which readily dissociates into I<sub>2</sub> and H<sub>2</sub> with laser or x-ray overexposure, has hindered experimental studies at high pressures. Currently there are no high-pressure studies at room temperature, nor any x-ray structural characterization at any temperature. The stability field of the compound at high pressure has been assumed and extrapolated based on the limited low-pressure, low-temperature data and the behavior of the other hydrogen halides, HCl and HBr [7,17].

Here we present high-pressure Raman spectroscopy and x-ray diffraction experiments exploring the formation, stability field, and structures of hydrogen iodide (HI). In addition to the three known solid configurations of HI, we present evidence for a phase I' at room temperature, structurally similar to cubic phase I, but differing in hydrogen atom distribution about the iodine atoms. A series of isothermal compressions between 300 K provide constraints on the phase diagram of HI and we find that at high pressures HI is unstable with respect to dissociation into its constituent elements thus ruling out the earlier claims of pressure-induced metallization of HI.

**II. METHODS**

Samples of HI were synthesized in diamond-anvil cells by the direct reaction between solid I<sub>2</sub> and fluid H<sub>2</sub>. Diamond anvils with 150–250  $\mu\text{m}$  culets were used for experiments, giving sample chamber diameters of between 75–100  $\mu\text{m}$ . Various concentrations of I<sub>2</sub> were loaded in an Ar-atmosphere glove box, with a small chip of ruby or gold as a pressure calibrant [20,21]. High-purity (99.9%) H<sub>2</sub> was subsequently gas loaded at 0.2 GPa. Reaction of H<sub>2</sub> and I<sub>2</sub> to produce HI occurs spontaneously with time at this low pressure, or can be accelerated by irradiation with up to 200 mW of 532 nm laser light. Samples were left for 24 h to equilibrate resulting in a mixture of two fluids exhibiting clear phase

\*ross.howie@hpstar.ac.cn

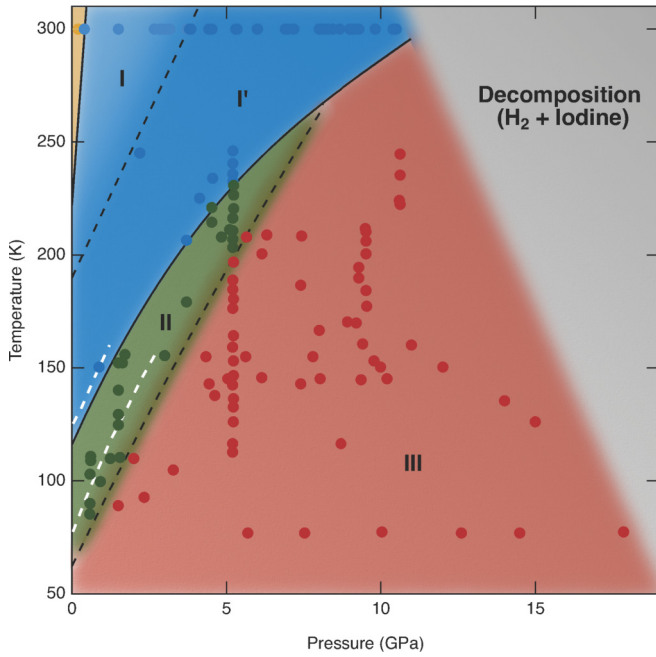


FIG. 1.  $P$ - $T$  phase diagram of HI. The yellow circle represents the liquid phase. Blue, dark blue, green, and red circles represent solid phases I, I', II, and III, respectively. The gray area indicates the  $P$ - $T$  conditions of dissociation. The phase I-I' and II-III boundaries are shown as dashed lines due to the significant overlap and ambiguity in the Raman spectra between phases. The white dashed lines show the I-II and II-III phase boundaries from Ref. [7].

separation. This process is only possible below 1 GPa, with the mixture remaining as I<sub>2</sub> and H<sub>2</sub> above this. Additionally, there would be no reformation if HI is dissociated through x-ray or laser overexposure. By careful control of the H<sub>2</sub> : I<sub>2</sub>

ratio, we were able to produce samples that were completely transformed to HI. Raman spectroscopy was used to test the purity of the prepared sample, showing trace amounts of both the constituent elements. Trace amounts of I<sub>2</sub> and H<sub>2</sub>, were also observed in previous studies where high purity HI was loaded directly [6,17].

Raman spectroscopy measurements were made using a custom-built microfocused Raman system. The laser power of the system was kept below 3 mW to prevent back transformation of the HI sample to I<sub>2</sub> and H<sub>2</sub> and laser exposure minimized to 0.2 s. We have found that above 1–2 GPa, photodissociation of I<sub>2</sub> is not possible with 200 mW of 532 nm laser light. X-ray diffraction data were collected at beam lines BL10XU, SPring-8, Japan and P02.2 ECB, PETRA, Germany [22,23]. Angle-dispersive x-ray diffraction patterns were recorded on PerkinElmer XRD1621 and Marr345 image-plate detectors with microfocused synchrotron radiation sources with energies in the range 30–43 keV. Two-dimensional image-plate data were integrated with DIOPTAS [24] to yield intensity vs  $2\theta$  plots. Patterns were indexed with DICVOL06 [25], Le Bail [26], and Rietveld [27] refinements were carried out in JANA2006 [28].

Exposure of HI to synchrotron x-ray radiation forms I<sub>2</sub>, which contaminates the resulting diffraction pattern with numerous peaks and requires acquiring data from a new sample and/or sample position at each pressure point. Typically HI crystallizes into large single-crystal domains within the sample chamber allowing diffraction spots from HI to be easily distinguished from the powder diffraction lines due to I<sub>2</sub>.

### III. RESULTS

The pressure-temperature phase and kinetic diagram between temperatures of 300 K and 77 K is shown in Fig. 1. The vibrational modes in solid HI, as with the other hydrogen

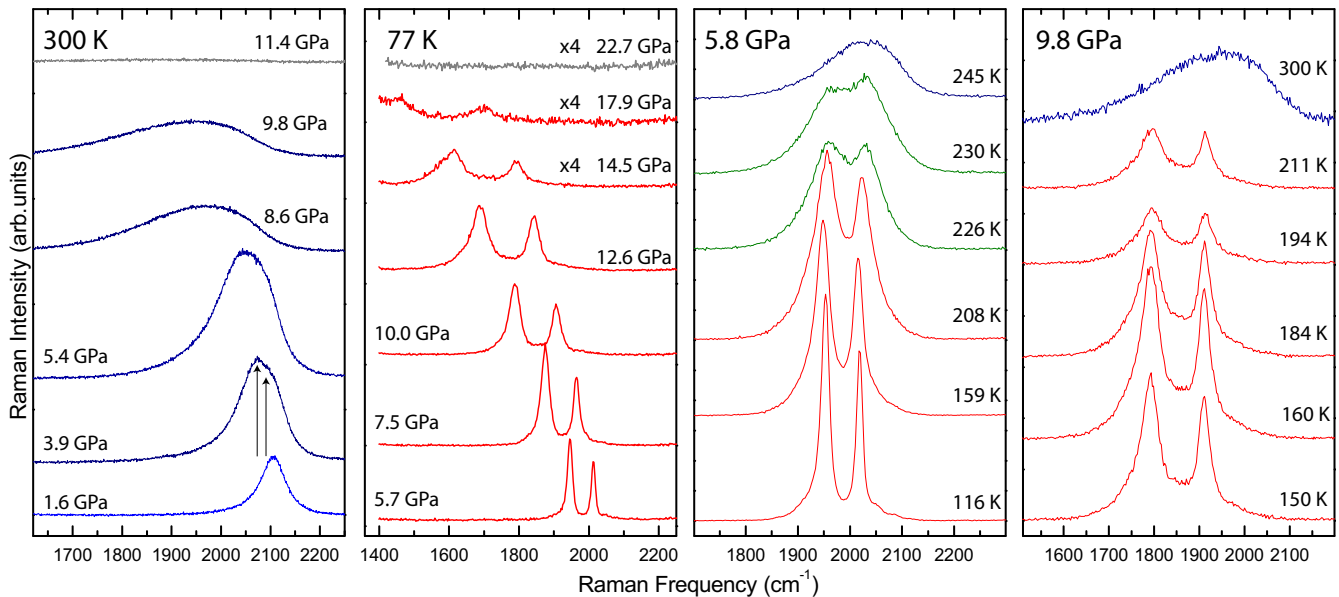


FIG. 2. Representative Raman spectra of an isothermal compression at 300 K (left panel), isothermal compression at 77 K (center left panel), an isobaric cooling/heating cycle at 5.8 GPa (center right panel) and an isobaric cooling/heating cycle at 9.8 GPa (right panel). Color indicates phases corresponding to the phase diagram in Fig. 1: light blue, phase I; dark blue, phase I'; green, phase II; red, phase III; and gray represents decomposition. Arrows indicate splitting of vibrational modes from phase I to I'.

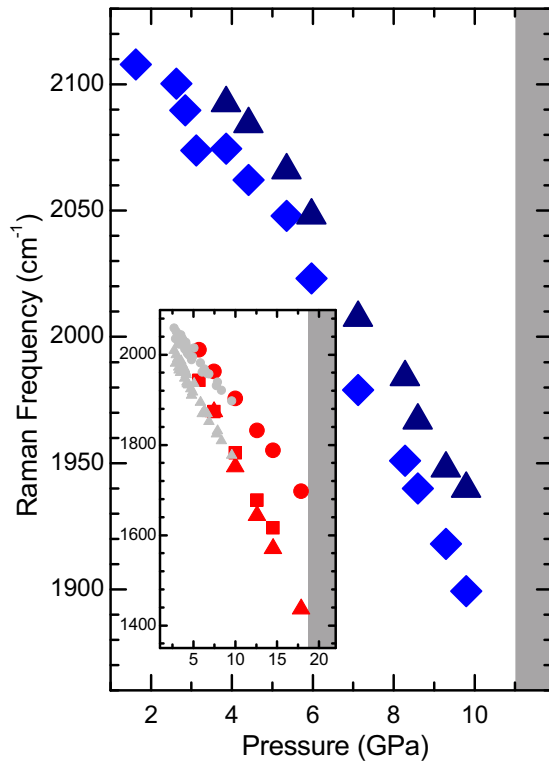


FIG. 3. Vibrational frequencies of HI on compression at 300 K, dark blue triangles indicate appearance of a second mode indicative of phase I'. Inset: Vibrational frequencies of HI on compression at 77 K, red points are from this study, while light gray points are taken from Ref. [7]. Dark gray shaded area indicates the pressure regime of decomposition

halides are due to the intramolecular H-X bond. The vibrational modes soften in the solid phase and at high pressures when intermolecular distances reduce and the strength of intermolecular interactions increases. At room temperature, the liquid phase is characterized by one symmetric vibrational mode at approximately  $2110 \text{ cm}^{-1}$ . On solidification to phase I, there is a significant broadening and softening of the mode (see Figs. 2 and 3). Despite numerous overlapping peaks, crystallization into phase I ( $Fm\bar{3}m$ ) was confirmed by x-ray diffraction measurements (Fig. 4).

Above pressures of 3.8 GPa at 300 K, the vibrational mode of HI shows a clear splitting into two modes, separated by  $20 \text{ cm}^{-1}$ . This same splitting was observed in HBr at pressures above 2.4 GPa at 295 K and interpreted to be a transition to a phase I' [12,16]. In HBr this transition is due to a rearrangement of the H-atom distribution with no change to the underlying fcc bromine-atom lattice of phase I, with associated symmetry change to  $Pa\bar{3}$ . Due to the weak x-ray scattering of H we cannot distinguish the two phases on the basis of x-ray diffraction alone. However, based on the close resemblance of the Raman spectra we propose a similar structure for HI phase I' (Fig. 4). Interestingly, phase I' is not seen in either DBr or HCl, suggesting that this phase is only observed in the heavier hydrogen halides.

On compression above 3.8 GPa, the asymmetry of the phase I' vibrational band increases and there is significant broadening of both modes. The frequencies of the vibrational

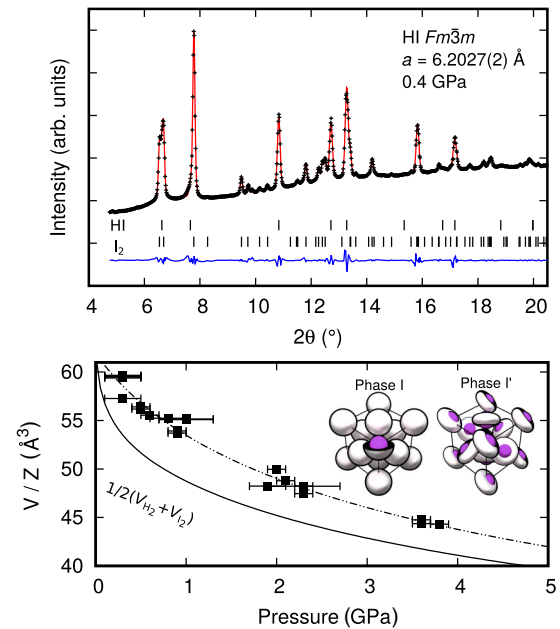


FIG. 4. (Top) Diffraction pattern of HI at 0.4 GPa, Le Bail profile refinement shown in red, difference shown in blue ( $wR_p = 1.68\%$ ); (bottom) HI equation of state, symbols are experimental data from individual runs. Dashed line corresponds to the calculated Birch-Murnaghan equation of state [HI:  $V_0 = 248(5) \text{ \AA}^3$ ,  $K_0 = 4.7(12) \text{ GPa}$ ,  $K_p = 5.2(11)$ ], solid line corresponds to the volume derived from the corresponding atomic equations of state of  $\text{I}_2$  [18] and  $\text{H}_2$  [19]. Inset: In phase I, hydrogen atoms freely rotate about iodine atoms (purple) represented by a shell model (white), phase I' exhibits a toroidal distribution of disordered hydrogen atom positions oriented along the  $\langle 111 \rangle$  cubic axes.

band decrease rapidly with pressure at a rate of  $-30 \text{ cm}^{-1}/\text{GPa}$  and extrapolating the frequencies would give a pressure of 69 GPa when the frequencies would reach zero (see Figs. 2 and 3). However, the intensity of the band starts to decrease above 6 GPa and by 11 GPa the HI vibrational mode disappears completely. This, together with the increase in intensity of the Raman modes of the constituent elements  $\text{H}_2$  and  $\text{I}_2$ , and sample darkening, are clear indicators of sample dissociation. This was confirmed by x-ray diffraction patterns from samples precompressed to above 11 GPa, which showed peaks due only to  $\text{I}_2$ . Once dissociation has taken place the sample remains as  $\text{I}_2$  and  $\text{H}_2$ , with no indication of further reaction in both Raman spectroscopy and x-ray diffraction measurements. On decompression after dissociation, there is no reformation of HI.

Each of the solid phases of HI at low temperature can be characterized by distinct vibrational Raman spectra, which can be correlated to the ambient pressure neutron diffraction data [11,29]: phase I, a symmetric broad stretching mode; phase I', a broad asymmetric doublet with separation of  $20 \text{ cm}^{-1}$ ; phase II, two broad overlapping modes with near equal intensity and separation of approximately  $65 \text{ cm}^{-1}$ ; and phase III, two sharp and distinct stretching modes (see right panel of Fig. 2). On isobaric cooling cycles we see that the phase I(I')-II-III transition sequence is completely reversible. On entering phase II from phase I or I', the vibrational mode

abruptly splits into two equally intense overlapping modes with separation of approximately  $80\text{ cm}^{-1}$ . Phase II is stable over a small  $P$ - $T$  regime, much like the other hydrogen halide HBr [16].

The gradual change in appearance of the vibrational modes of phase II with pressure/temperature results in some ambiguity as to at which temperatures the phase II to III transition occurs. The doublet separation gradually gets larger, each mode decreases in width, and the lower frequency mode surpasses the intensity of the higher frequency mode (see Fig. 2). On compression of phase III at 77 K, we see the similar behavior observed with the vibrational modes at room temperature: rapid softening, a fourfold increase in width, and by 17 GPa, a 95% reduction in intensity of the HI vibrons compared to 5 GPa. In phase III each vibrational mode shifts at a different rate,  $-26\text{ cm}^{-1}/\text{GPa}$  and  $-42\text{ cm}^{-1}/\text{GPa}$ . HI is slightly more stable at low temperature, with dissociation occurring above 18 GPa.

#### IV. DISCUSSION AND CONCLUSIONS

Despite the sensitivity to decomposition it was previously assumed that HI would remain stable up to very high pressures and enter a metallic state at low temperature [6,7]. Metallization was initially inferred by the extrapolation of absorption measurements conducted at pressures below 25.5 GPa, i.e., below the conditions at which we report dissociation. Subsequent electrical conductivity measurements carried out on a single sample show sharp drops in resistivity at 42 and 51 GPa. These drops are interpreted as a molecular-insulator to molecular-conductor transition followed by transition to a metallic state. Other conductivity measurements presented in Ref. [6] clearly correspond to the metallization of  $\text{I}_2$  occurring at 16 GPa [30,31]. Both diagnostic techniques used in these early studies do not probe either the crystal structure or molecular behavior at high pressures, meaning that dissociation—a simpler explanation of the experimental results—was overlooked. Our combined x-ray diffraction and Raman spectroscopy measurements demonstrate that (metallic) HI cannot be present at the corresponding temperatures and pressures reported in Refs. [6,7]. The dissociation pressures of the hydrogen halides decrease down the period (HBr has been

shown to dissociate at pressures above 42 GPa and HCl shown to be stable to at least 50 GPa), it can therefore be expected that the heavier hydrogen halide would dissociate at a much lower pressure [32].

At pressures close to ambient, the volume of HI (Fig. 4, bottom panel) is approximately equal to the combined volumes of  $\text{H}_2$  and  $\text{I}_2$ . However, the high compressibility of hydrogen leads to an increasing difference between these volumes at higher pressure, whereby the experimental determined value is greater than the calculated value up to 9 GPa at 300 K. This implies that HI is unstable with respect to its constituent elements. Having the longest bond ( $1.60\text{ \AA}$  vs  $1.43\text{ \AA}$  in DBr and  $1.28\text{ \AA}$  in DCl) HI is the least stable among these compounds. It appears that the decomposition of HI upon compression is not due to the intrinsic elastic or dynamical instability, e.g., HBr and HCl are stable to much higher pressures. An intrinsic stability limit is defined by the decrease in HI bonding strength therefore preventing the formation of phases with stoichiometry other than 1 : 1. This observation raises an interesting question about the predicted superconducting phases of the hydrogen iodide compounds with stoichiometry other than 1 : 1.  $\text{H}_2\text{I}$  and  $\text{H}_4\text{I}$  are both suggested to be superconducting at pressures of 100 GPa but are unlikely to be stable with respect to decomposition to their constituent elements at such conditions [8,9]. This may also hold true for the superconducting phases of HCl and HBr predicted at pressures of 280 GPa and 160 GPa, respectively [33]. At pressures up to 60 GPa and at temperatures of 80 K and 300 K, we observed no further reaction between  $\text{H}_2$  and  $\text{I}_2$ , suggesting that much higher pressures and most probably high temperature to overcome the kinetic barrier would be required to promote formation of any the theoretically predicted  $\text{H}_2\text{-I}_2$  compounds [8,9].

#### ACKNOWLEDGMENTS

This work was supported by the NSF of China (Grant No. 11404343), Natural Science Foundation of Anhui Province, China (Grant No. 1508085QA07). Parts of this research were carried out at P02.2 at DESY, a member of the Helmholtz Association (HGF). We would like to thank H.-P. Liermann and K. Glazyrin for assistance. Part of this work was performed under Proposal No. 2017A1062 at SPring-8.

- 
- [1] E. Wigner and H. B. Huntington, *J. Chem. Phys.* **3**, 764 (1935).
  - [2] M. Eremets and I. Troyan, *Nat. Mater.* **10**, 927 (2011).
  - [3] R. T. Howie, C. L. Guillaume, T. Scheler, A. F. Goncharov, and E. Gregoryanz, *Phys. Rev. Lett.* **108**, 125501 (2012).
  - [4] P. Dalladay-Simpson, R. T. Howie, and E. Gregoryanz, *Nature (London)* **529**, 63 (2016).
  - [5] A. P. Drozdov, M. I. Eremets, I. A. Troyan, V. Ksenofontov, and S. I. Shylin, *Nature (London)* **525**, 1 (2015).
  - [6] J. van Straaten and I. F. Silvera, *Phys. Rev. Lett.* **57**, 766 (1986).
  - [7] J. van Straaten and I. F. Silvera, *Phys. Rev. B* **36**, 9253 (1987).
  - [8] A. Shamp and E. Zurek, *J. Phys. Chem. Lett.* **6**, 4067 (2015).
  - [9] D. Duan, F. Tian, Y. Liu, X. Huang, D. Li, H. Yu, Y. Ma, B. Liu, and T. Cui, *Phys. Chem. Chem. Phys.* **17**, 32335 (2015).
  - [10] E. Sándor and R. F. C. Farrow, *Nature (London)* **14**, 171 (1967).
  - [11] A. Ikram, B. H. Torrie, and B. M. Powell, *Mol. Phys.* **79**, 1037 (1993).
  - [12] J. K. Cockcroft, A. Simon, and K. R. A. Ziebeck, *Z. Kristallogr.* **184**, 229 (1988).
  - [13] E. Sándor and M. W. Johnson, *Nature (London)* **217**, 542 (1968).
  - [14] E. Sándor and R. F. C. Farrow, *Discuss. Faraday Soc.* **48**, 78 (1969).
  - [15] W. Y. Zeng, Y. Z. Mao, and A. Anderson, *J. Raman Spectrosc.* **30**, 995 (1999).
  - [16] T. Kume, T. Tsuji, S. Sasaki, and H. Shimizu, *Phys. Rev. B* **58**, 8149 (1998).
  - [17] J. van Straaten and I. F. Silvera, *Phys. Rev. B* **36**, 9301 (1987).
  - [18] K. Takemura, S. Minomura, O. Shimomura, Y. Fujii, and J. D. Axe, *Phys. Rev. B* **26**, 998 (1982).

- [19] P. Loubeyre, R. LeToullec, D. Hausermann, M. Hanfland *et al.*, *Nature (London)* **383**, 702 (1996).
- [20] H. K. Mao, J. Xu, and P. M. Bell, *J. Geophys. Res.* **91**, 4673 (1986).
- [21] Y. Fei, A. Ricolleau, M. Frank, K. Mibe, G. Shen, and V. Prakapenka, *Proc. Nat. Acad. Sci. USA* **104**, 9182 (2007).
- [22] Y. Ohishi, N. Hirao, N. Sata, K. Hirose, and M. Takata, *High Press. Res.* **28**, 163 (2008).
- [23] H.-P. Liermann, Z. Konôpková, W. Morgenroth, K. Glazyrin, J. Bednarčík, E. McBride, S. Petitgirard, J. Delitz, M. Wendt, Y. Bican *et al.*, *J. Sync. Rad.* **22**, 908 (2015).
- [24] C. Prescher and V. B. Prakapenka, *High Press. Res.* **35**, 223 (2015).
- [25] A. Boultif and D. Louër, *J. Appl. Crystallogr.* **37**, 724 (2004).
- [26] A. Le Bail, H. Duroy, and J. Fourquet, *Mater. Res. Bull.* **23**, 447 (1988).
- [27] H. M. Rietveld, *J. Appl. Crystallogr.* **2**, 65 (1969).
- [28] V. Petříček, M. Dušek, and L. Palatinus, *Z. Kristallogr.* **229**, 345 (2014).
- [29] A. Anderson, B. H. Torrie, and W. S. Tse, *J. Raman Spectrosc.* **8**, 213 (1979).
- [30] A. S. Balchan and H. G. Drickamer, *J. Chem. Phys.* **34**, 1948 (1961).
- [31] N. Sakai, K. Takemura, and K. Tsuji, *J. Phys. Soc. Jpn.* **51**, 1811 (1982).
- [32] E. Katoh, H. Yamawaki, H. Fujihisa, M. Sakashita, and K. Aoki, *Phys. Rev. B* **59**, 11244 (1999).
- [33] D. Duan, F. Tian, Z. He, X. Meng, L. Wang, C. Chen, X. Zhao, B. Liu, and T. Cui, *J. Chem. Phys.* **133**, 074509 (2010).